Generalized hydrodynamics and Reynolds-number dependence of steady-flow properties in the cylindrical Couette flow of Lennard-Jones fluids

Roger E. Khayat and Byung Chan Eu*
Department of Chemistry, McGill University, 801 Sherbrooke Street West, Montreal, Quebec, Canada H3A 2K6
(Received 16 November 1988; revised manuscript received 1 February 1989)

The Reynolds-number dependence is calculated for the shear stress, normal stress difference, velocity, effective viscosity, and effective normal stress coefficient by using the generalized hydrodynamic equations in the case of cylindrical Couette flow of a Lennard-Jones gas. The drag coefficient is shown to decrease more rapidly than the inverse Reynolds number and rapidly vanish on passing a critical Reynolds number. The shear stress and normal stress difference also vanish beyond the critical Reynolds number, and there is a region in space where the effective shear viscosity and normal stress coefficients become so small that the fluid behaves like an almost inviscid fluid in the region. These numerical results indicate that the generalized hydrodynamic equations tend to the Euler equations in the limit of sufficiently large Reynolds number at a rate faster than that for the Navier-Stokes equation and that the fluid is almost inviscid in some parts where the velocity changes steeply, and viscous in the rest.

I. INTRODUCTION

In the Navier-Stokes theory of fluid dynamics the effects of viscosity is accounted for by the term $-\eta_0\nabla^2\mathbf{u}$, where η_0 is the viscosity coefficient and $\mathbf{u}$ is the fluid velocity. When cast in reduced form, this term is multiplied by the inverse Reynolds number $\mathcal{N}_{\mathrm{Re}}^{-1}$, while the rest of the momentum balance equation—i.e., the Navier-Stokes equation—is the order of unity with respect to $\mathcal{N}_{\mathrm{Re}}$. Therefore the importance of the viscous term diminishes as $\mathcal{N}_{\mathrm{Re}}$ increases, and the Navier-Stokes equation asymptotically approaches the Euler equation for ideal fluids. It turns out that the reduced stress is $O(1)$ in the flow geometry considered in the present work, and therefore does not change as the flow conditions, such as the density and the reference velocity—e.g., the mean velocity or the mainstream velocity—vary. This feature is an important characteristic of the Navier-Stokes equation in the present geometry.

When the stress tensor is proportional to the velocity gradient, as in the Navier-Stokes theory, the fluid is said to be Newtonian, but fluids are generally Newtonian only if the shear rate is sufficiently small, and become non-Newtonian, that is, the viscosity is dependent on the shear rate, as the shear rate increases to a large value. An interesting example is the molecular-dynamics calculations[1] on argon, which show that even argon, which is a typical simple fluid, becomes a non-Newtonian fluid as its density and temperature reach those of the triple point and the shear rate increases to a sufficiently large value. Non-Newtonian fluids are generally known to have a high value for the zero-shear-rate viscosity. However, in the case of argon, since the potential energy of interaction is rather small, its Newtonian viscosity η_0 is also quite small, and yet it can become non-Newtonian under such conditions. This strongly suggests that all fluids can generally become non-Newtonian when they reach a state in which their constitutive equation for their stress tensor becomes nonlinear with respect to the velocity gradient and/or stress tensor, and therefore the viscosity is shear-rate dependent. If this is the case, then the viscous term in the Navier-Stokes equation must be replaced by $\nabla\cdot\vec{\vec{\Pi}}$, where $\vec{\vec{\Pi}}$ is the stress tensor given by a nonlinear constitutive equation, and, when cast in a suitable reduced form, $\nabla^*\cdot\vec{\vec{\Pi}}^*$ in the present geometry is expected to be no longer $O(1)$ with respect to $\mathcal{N}_{\mathrm{Re}}$, but a function of $\mathcal{N}_{\mathrm{Re}}$ whose precise form is determined by the solution of the constitutive equation for $\vec{\vec{\Pi}}$ and the momentum balance equation. In this paper we investigate the Reynolds-number dependence of shear stress and normal stress differences of a Lennard-Jones fluid in the case of cylindrical Couette flow, by using generalized hydrodynamic equations.[2,3]

In the previous papers[2–4] on cylindrical Couette flow of a Lennard-Jones gas, we have used a steady generalized hydrodynamic equations derived from the Boltzmann equation. When appropriately cast into similarity forms by using reduced variables, the generalized hydrodynamic equations contain, in addition to the Prandtl and Eckert numbers associated with heat transfer between the gas and the walls, two important fluid dynamical numbers, Reynolds (or Mach) and Knudsen numbers, and the dependence on the latter of flow properties has been the focus of interest in our previous work.[2–4] Since the available experimental data were obtained for various values of the Knudsen number at a fixed Mach, Prandtl, and Eckert number, the generalized hydrodynamic equations were numerically solved only for cases corresponding to the experimental conditions at a fixed Mach number. The results of calculation are in good agreement with experiment and the Monte Carlo direct simulation results, and have been reported.[2–4] The reduced generalized hydrodynamic equations used for the purpose suggest that they should reduce to the

corresponding set of Euler's (ideal) hydrodynamic equations at a rate different from that predicted by the Navier-Stokes equation as the Reynolds number increases. In the present paper we address our inquiry to this question and report on the salient features of our study on the Reynolds-number dependence of the shear stress, normal stress differences, and related quantities in the case of cylindrical Couette flow. From the $\mathcal{N}_{\mathrm{Re}}$ dependence calculated, we may make some inference on the approach of the generalized hydrodynamic equations to Euler's equations, at least, in the case of the flow under consideration.

The Navier-Stokes equation contains a constant viscosity coefficient as a constitutive parameter. Since the viscosity of a gas of normal density is independent[5] of the gas density, the Navier-Stokes equation becomes incapable of describing the gas behavior in the low-density regime, where the viscosity vanishes with the diminishing density of the gas. This low-density difficulty is a major weakness of the Navier-Stokes theory, which is usually avoided by modifying the boundary conditions in the conventional methods[6] in rarefied gas dynamics. However, such modifications yield only adjustable parameter theories, since they contain accommodation coefficients which are adjustable parameters in practice. In the previous papers[2-4] on cylindrical Couette flow of a Lennard-Jones gas, we have shown that generalized hydrodynamic equations can explain experimental data on a low-density gas without modifying the boundary conditions from stick to slip boundary conditions, provided nonlinear transport processes are appropriately taken into consideration. The nonlinear transport processes and the terms in the generalied hydrodynamic equations yield an entropy production qualitatively different[7] from the linear irreversible thermodynamic form (i.e., the Rayleigh-Onsager dissipation function[8]). Since they are also largely responsible for providing the features missing in the Navier-Stokes and Fourier equations, they provide a logical object of investigation to answer the question posed above. We have previously shown[2,3] that the same terms provide a way to avoid the aforementioned difficulty with the Navier-Stokes equation in gas dynamics. Therefore, answering the question regarding the $\mathcal{N}_{\mathrm{Re}}$ dependence of flow properties would, simultaneously, answer whether the scope of generalized hydrodynamic equations can cover a wider range of fluid density and thermodynamic forces within a single framework of theory. Moreover, understanding the manner in which inviscid fluid behavior is approached by a fluid as the Reynolds number increases, may also provide some clues to how a turbulent fluid behavior might arise in a fluid flow since turbulence occurs beyond a sufficiently large Reynolds number. In this connection it is useful to refer to a recent work by Hellberg and Orszag,[9] who have studied instability of a three-mode projection of the Navier-Stokes equation and found that decreasing the viscosity below a critical value is accompanied by period-doubling bifurcations by the flow. It is interesting that these authors elect to change the viscosity instead of simply increasing the Reynolds number. However, it must be noted that changing the viscosity in the Navier-Stokes equation is equivalent to changing the substance to another, since the viscosity is invariant in the Navier-Stokes equation, and consequently, the effect of the change in viscosity is seen only over a class of substances but not in a particular substance undergoing the flow under consideration. In generalized hydrodynamics an effective viscosity appears in the place of η_0 (Newtonian viscosity). Therefore it is interesting to examine a mode by which the effective viscosity locally changes in a given substance. As we will see, the generalized hydrodynamics approach does not require changing the substance to vary the effective viscosity. The nonlinear transport processes in the flow automatically take care of that, since the effective viscosity can be a strong function of position, and thus significantly deviate from the zero-shear-rate viscosity (i.e., Newtonian viscosity) as the position changes. Under these circumstances the question addressed here becomes quite interesting and may even have a deeper meaning to fluid dynamics in general, since the fluid over a volume may appear to be a spatially inhomogeneous blend of almost inviscid and viscous fluids, the inviscid part arising from the rapidly changing velocity field while the viscous part arising from the slowly changing velocity field.

Here we examine, in particular, the Reynolds-number dependence of shear stress and normal stress differences along with the velocity, shear viscosity, normal stress coefficient, and drag coefficient for cylindrical Couette flow of a Lennard-Jones gas. We find them rapidly decreasing in general, and eventually vanishing altogether, except for the transport coefficients which attain a constant value, as the Reynolds number increases beyond a critical value. In our previous studies we have made anticipatory remarks without proof or concrete evidence regarding the asymptotic approach to the Euler equations taken by the generalized hydrodynamic equations. The flow behavior mentioned above confirms our anticipation, and here we provide a piece of evidence for such behavior.

In Sec. II we present a short summary of generalized hydrodynamic equations for the flow problem in equation and in Sec. III the numerical results are presented for flow profiles and the Reynolds-number dependence of shear stress, primary normal stress difference (the secondary normal stress coefficient is equal to the negative of the primary one in the present theory), and drag coefficient. Section IV is for concluding remarks.

II. GENERALIZED HYDRODYNAMIC EQUATIONS: A BRIEF SUMMARY

In a macroscopic description of irreversible processes we aim to obtain a theory completely consistent with the thermodynamic laws, since no irreversible process is possible if it violates the thermodynamic laws. If we start the description from a statistical-mechanical—namely, kinetic—theory of matter, then the evolution equations derived from the kinetic equation must be made consistent with the statistical-mechanical representation of the second law in particular. In the modified moment method[7(a),7(b),10(a)] of solution for the Boltzmann equation and generalized Boltzmann equation[10(b)] for dense

fluids, approximate solutions to the kinetic equation are obtained in such a way that the H theorem is satisfied by them. Since the evolution equations for macroscopic variables necessary for describing a process of interest are derived with such an approximate solution, they are fully consistent with the thermodynamic laws, and we are assured that physical deductions we make from the evolution equations so obtained are also consistent, at least, with the important second law of thermodynamics.

The modified moment method[7(a),7(b),10] yields a set of evolution equations for macroscopic variables, which generalize the conventional hydrodynamic equations. The evolution equations consist of the usual conservation equations and constitutive equations for fluxes. The latter consist of terms collectively called the convective term, which contains the thermodynamic force driving the particular flux, and a term that we call the dissipative term. This term originates from the collision term in the kinetic (i.e., Boltzmann) equation and is the seat of energy dissipation. The derivatives of constitutive equations that we use in practice involve an approximation for the nonlinear collision integral in the Boltzmann equation, or the generalized Boltzmann equation, but the approximation does not involve a linearization of the collision integral. This feature is an important one that sets the modified moment method apart from the Chapman-Enskog method[5] of solution, or the conventional moment method.[11] To obtain such an approximation we use a cumulant expansion method for the collision integral, and, to first-order cumulant approximation, the collision integral yields dissipative terms in the constitutive equations for fluxes which are proportional to a hyperbolic sine function whose argument is simply the Rayleigh-Onsager dissipation function. Therefore, the cumulant expansion yields dissipative terms that amount to a partial resummation of infinite Chapman-Enskog series for the collision term in the Boltzmann equation. The constitutive equations thus obtained are expected to be better behaved, but they are highly nonlinear with respect to fluxes

A. Generalized hydrodynamic equations for a single-component fluid

To such an approximation, and to the usual 13-moment approximation,[12] the set of evolution equations is as follows:

$$\frac{\partial}{\partial t}\rho(\mathbf{r},t)=-\nabla\cdot\rho\mathbf{u}(\mathbf{r},t)\ , \tag{1}$$

$$\rho\frac{d}{dt}\mathbf{u}(\mathbf{r},t)=-\nabla\cdot\vec{\mathbf{P}}(\mathbf{r},t)\ , \tag{2}$$

$$\rho\frac{d}{dt}\mathcal{E}(\mathbf{r},t)=-\nabla\cdot\mathbf{Q}-\vec{\mathbf{P}}:\nabla\mathbf{u}\ , \tag{3}$$

$$\rho\frac{d}{dt}\hat{\vec{\mathbf{P}}}(\mathbf{r},t)=2p\vec{\gamma}+2\rho[\hat{\vec{\mathbf{P}}}\cdot\vec{\gamma}]^{(2)}-\rho[\vec{\omega},\hat{\vec{\mathbf{P}}}]-\frac{p\rho\hat{\vec{\mathbf{P}}}}{\eta_0}\frac{\sinh\kappa}{\kappa}\ , \tag{4}$$

$$\rho\frac{d}{dt}\hat{\mathbf{Q}}(\mathbf{r},t)=-(\nabla\cdot\vec{\mathbf{P}})\cdot\hat{\vec{\mathbf{P}}}+\mathbf{Q}\cdot\vec{\gamma}-\hat{C}_p\vec{\mathbf{P}}\cdot\nabla T-\rho[\vec{\omega},\hat{\mathbf{Q}}]-T\hat{C}_p\frac{p\rho\hat{\mathbf{Q}}}{\lambda_0}\frac{\sinh\kappa}{\kappa}\ , \tag{5}$$

$$\rho\frac{d}{dt}\hat{\Delta}(\mathbf{r},t)=\tfrac{2}{3}\rho\hat{\vec{\mathbf{P}}}:\vec{\gamma}-\tfrac{2}{3}\rho\hat{\Delta}\nabla\cdot\vec{\gamma}-\rho\frac{d}{dt}\ln(pv^{5/3})-\frac{p\rho\hat{\Delta}}{\eta_{b0}}\frac{\sinh\kappa}{\kappa}\ , \tag{6}$$

where the flux evolution equations are in the Jaumann derivative form, whose kinetic theory basis is discussed in Refs. 12 and 13. In (1)–(6) d/dt is the substantial derivative, ρ is the mass density, $v=1/\rho$ is the specific volume, $\mathbf{u}$ is the fluid velocity, $\mathcal{E}$ is the internal energy, $\hat{C}_p$ is the specific heat per unit mass, $\vec{\mathbf{P}}$ is the stress tensor, $\mathbf{Q}$ is the heat flux, p is the hydrostatic pressure,

$$\vec{\gamma}=-\tfrac{1}{2}[\nabla\mathbf{u}+(\nabla\mathbf{u})^t]+\tfrac{1}{3}\vec{U}\nabla\cdot\mathbf{u}\ ,$$

$$\vec{\omega}=\tfrac{1}{2}[\nabla\mathbf{u}-(\nabla\mathbf{u})^t]\ ,$$

$$\hat{\vec{\mathbf{P}}}=[\tfrac{1}{2}(\vec{\mathbf{P}}+\vec{\mathbf{P}}^t)-\tfrac{1}{3}\vec{U}\,\mathrm{tr}\vec{\mathbf{P}}]/\rho\ ,$$

$$\hat{\Delta}=(\tfrac{1}{3}\mathrm{tr}\vec{\mathbf{P}}-p)/\rho\ ,$$

$$\hat{\mathbf{Q}}=\mathbf{Q}/\rho\ ,$$

$$[\vec{\omega},A]=\vec{\omega}\cdot A-A\cdot\vec{\omega}\ ,$$

$$\kappa=\rho[(\tau_p/2\eta_0)^2\hat{\vec{\mathbf{P}}}:\hat{\vec{\mathbf{P}}}+(\tau_b/\eta_{b0})^2\hat{\Delta}^2+(\tau_q/\lambda_0)^2\hat{\mathbf{Q}}\cdot\hat{\mathbf{Q}}]^{1/2}\ ,$$

$$\tau_p=[2\eta_0(m_r k_B T/2)^{1/2}]^{1/2}/nk_BT\sigma\ ,$$

$$\tau_q=[\lambda_0(m_r k_B T/2)^{1/2}]^{1/2}/nk_BT\sigma\ ,$$

$$\tau_b=[\eta_{b0}(m_r k_B T/2)^{1/2}]^{1/2}/nk_BT\sigma\ .$$

Here η_0 is the Newtonian viscosity, λ_0 is the Fourier thermal conductivity, η_{b0} is the bulk viscosity, m_r is the reduced mass, n is the number density, σ is the size parameter of the molecule, k_B is the Boltzmann constant, and $\vec{U}$ is the unit second-rank tensor.

The set of evolution equations (1)–(6), which we will call generalized hydrodynamic equations, is closed except for the equation of state and the caloric equation of state necessary for the pressure and the specific heat in the evolution equations, and their solutions subject to boundary and initial conditions will enable us to describe flow properties of a substance of interest. The first three equations (1)–(3) are familiar conservation laws for mass, momentum, and internal energy. The last three equations (4)–(6) are the constitutive equations for the traceless symmetric part of the stress tensor, its excess trace part, and the heat flux of the substance. These constitutive equations contain information on the molecular constitution of the substance in the transport coefficients—viscosity, bulk viscosity, and thermal conductivity—appearing in them. Except for these, the parameters τ_p, τ_b, and τ_q and the specific heat, no other variables in the set (1)–(6) reflect the molecularity of the substance in

question. It is significant that the molecular parameters appear in the dissipative terms—i.e., the terms involving the hyperbolic sine function—in (4)–(6). Thus we see that energy dissipation is a result of molecular interactions in the system. The dissipative terms in the constitutive equations are directly associated with the entropy production occurring in the system because of the dissipative fluxes present in the system: momentum fluxes (stress tensors), heat fluxes, and diffusion fluxes in the case of a mixture. The entropy production is in fact given by the formula

$$\sigma_{\text{ent}}=k_B g^{-1}\kappa\sinh\kappa \ , \tag{7}$$

where

$$g=(m_r/2k_BT)^{1/2}/(n\sigma)^2 \ .$$

This form of entropy production is always positive and reduces to the Rayleigh-Onsager dissipation function appearing in linear irreversible thermodynamics holding near equilibrium. Therefore the irreversible processes described by (4)–(6) may be regarded as occurring far from equilibrium, in the sense that the entropy production (7) reduces to its linear-theory version as the values of the fluxes get small.

Since we will consider gases with no bulk viscosity, we may set $\hat{\Delta}=0$ and neglect (6) entirely. We must add to the set (1)–(6) an equation of state, as well as the caloric equation of state for the specific heat. In our calculation below we will take the ideal-gas versions for them.

The reader is referred to the previous papers[2,3] in this series for a discussion on the significance of the Jaumann derivatives and corotational formulation of constitutive equations. The kinetic equations, such as the Boltzmann equation for dilute gases and the generalized Boltzmann equation for dense fluids, produce constitutive equations containing higher-order moments. The latter are neglected in (4)–(6), since the number of moments is limited to 13 in the present theory. We believe that it makes more sense to simply neglect the higher moments than to calculate them in terms of lower-order moments, since the 13-moment approximation is equivalent to mutilating a mathematical space of macroscopic variables (Gibbs space) to a space of lower dimension, and it does not make sense to include variables in the subset truncated away in the approximation. Note, however, it is the conventional practice to include higher-order moments expressed in terms of lower-order moments in the usual moment method.[11]

B. Steady generalized hydrodynamic equations

Since we are interested in the cylindrical Couette flow of a Lennard-Jones gas, the most appropriate coordinate system is that of cylindrical coordinates (r,θ,z). We imagine that two concentric cylinders of a sufficiently long length are aligned along the z axis. The radii of the inner and outer cylinders are, respectively, R_i and R_o, and the inner cylinder rotates at angular speed Ω around the z axis. The inner and outer cylinders are at different temperatures T_i and T_o, respectively, and $T_o>T_i$. Therefore, there is a heat flow from the inner to the outer cylinder. To study this system it is convenient to express the generalized hydrodynamic equations in the cylindrical coordinates. For this purpose we first decompose various vectors and tensors into components:

$$\mathbf{u}=u_r\delta_r+u_\theta\delta_\theta+u_z\delta_z \ ,$$

$$\mathbf{Q}=Q_r\delta_r+Q_\theta\delta_\theta+Q_z\delta_z \ ,$$

$$\begin{aligned}\rho\hat{\mathbf{P}}\equiv\vec{\vec{\Pi}}=&\Pi_{rr}\delta_r\delta_r+\Pi_{r\theta}\delta_r\delta_\theta+\Pi_{rz}\delta_r\delta_z+\Pi_{\theta r}\delta_\theta\delta_r\\&+\Pi_{\theta\theta}\delta_\theta\delta_\theta+\Pi_{\theta z}\delta_\theta\delta_z+\Pi_{zr}\delta_z\delta_r+\Pi_{z\theta}\delta_z\delta_\theta\\&+\Pi_{zz}\delta_z\delta_z \ ,\end{aligned}$$

and similar decompositions can be made for tensors $\vec{\vec{\gamma}}$ and $\vec{\vec{\omega}}$. Here δ_r, δ_θ, and δ_z are unit vectors in the cylindrical coordinate system. The vector and tensor components u_r, Π_{rr}, etc. depend on r, θ, and z in general.

If we assume that the length of cylinders is infinite in order to remove the end effect, the system becomes translationally symmetric along the z axis. Consequently, the fluid properties are translationally invariant in z and the macroscopic variables become independent of z. Since there is also axial symmetry around the z axis, they are also independent of the angle variable θ. Thus the macroscopic variables depend on the radial position r only. Taking these symmetry properties into account, we obtain the steady-state equations for (1)–(5) in cylindrical coordinates in the following forms:[14]

$$\frac{d}{dr}(r\rho u_r)=0 \ , \tag{8}$$

$$\rho\left[u_r\frac{du_r}{dr}-\frac{u_\theta^2}{r}\right]=-\frac{d}{dr}(\rho+\Pi_{rr})-(\Pi_{rr}-\Pi_{\theta\theta})/r \ , \tag{9a}$$

$$\rho\left[u_r\frac{du_\theta}{dr}+\frac{u_ru_\theta}{r}\right]=-r^{-2}\frac{d}{dr}(r^2\Pi_{r\theta})+(\Pi_{r\theta}-\Pi_{\theta r})/r \ , \tag{9b}$$

$$\rho u_r\frac{du_z}{dr}=-r^{-1}\frac{d}{dr}(r\Pi_{rz}) \ , \tag{9c}$$

$$\begin{aligned}\rho u_r\frac{d\mathcal{E}}{dr}=&-r^{-1}\frac{d}{dr}(rQ_r)-\Pi_{\theta r}\frac{du_\theta}{dr}\\&-\Pi_{zr}\frac{du_z}{dr}+\frac{\Pi_{r\theta}u_\theta-(p+\Pi_{\theta\theta})u_r}{r}\\&-(p+\Pi_{rr})\frac{du_r}{dr} \ ,\end{aligned} \tag{10}$$

$$\begin{aligned}p\Pi_{rr}\frac{q_e}{\eta_0}=&-2p\gamma_r-\tfrac{8}{3}(\gamma\Pi_{r\theta}+\beta\Pi_{\theta z})\\&+\tfrac{2}{3}(\Pi_{\theta\theta}\gamma_\theta+\Pi_{zz}\gamma_z-2\Pi_{rr}\gamma_r)\\&-3\nu\Pi_{rr}-u_r\frac{d\Pi_{rr}}{dr} \ ,\end{aligned} \tag{11a}$$

$$p\Pi_{r\theta}\frac{q_e}{\eta_0}=-2p\gamma-2(\gamma\Pi_{\theta\theta}+\beta\Pi_{\theta z})+(\gamma_z-3\nu)\Pi_{r\theta} -u_r\frac{d\Pi_{r\theta}}{dr}\ , \tag{11b}$$

$$p\Pi_{\theta\theta}\frac{q_e}{\eta_0}=-2p\gamma_\theta+\tfrac{4}{3}(\gamma\Pi_{r\theta}+\beta\Pi_{rz}) +\tfrac{2}{3}(\Pi_{rr}\gamma_r+\Pi_{zz}\gamma_z-2\Pi_{\theta\theta}\gamma_\theta) -3\nu\Pi_{\theta\theta}-u_r\frac{d\Pi_{\theta\theta}}{dr}\ , \tag{11c}$$

$$p\Pi_{rz}\frac{q_e}{\eta_0}=-2p\beta-2(\gamma\Pi_{\theta z}+\beta\Pi_{zz})+(\gamma_\theta-3\nu)\Pi_{rz} -u_r\frac{d\Pi_{rz}}{dr}\ , \tag{11d}$$

$$p\Pi_{\theta z}\frac{q_e}{\eta_0}=(\gamma_r-3\nu)\Pi_{\theta z}-u_r\frac{d\Pi_{\theta z}}{dr}\ , \tag{11e}$$

$$p\Pi_{zz}\frac{q_e}{\eta_0}=-2p\gamma_z+\tfrac{4}{3}(\gamma\Pi_{r\theta}+\beta\Pi_{zr}) +\tfrac{2}{3}(\Pi_{rr}\gamma_r+\Pi_{\theta\theta}\gamma_\theta-2\Pi_{zz}\gamma_z)-3\nu\Pi_{zz} -u_r\frac{d\Pi_{zz}}{dr}\ , \tag{11f}$$

$$Q_rq_e=-\lambda_0\chi-\frac{\lambda_0}{\alpha}\left[(2\gamma+\omega)Q_\theta +\left(T\hat{C}_p\chi-\frac{u_\theta^2}{r}-\frac{u_r^2}{r}+3u_r\nu\right)\Pi_{rr} +3\beta Q_z+2\beta u_r\Pi_{rz}+2\omega u_r\Pi_{r\theta}\right] -(\gamma_r+3\nu)Q_r-u_r\frac{dQ_r}{dr}\ , \tag{12a}$$

$$Q_\theta q_e=-\frac{\lambda_0}{\alpha}\left(T\hat{C}_p\chi-\frac{u_\theta^2}{r}+3\nu u_r-\frac{u_r^2}{r}\right)\Pi_{\theta r} +\frac{\lambda_0}{\alpha}(\omega Q_r-2\omega u_r\Pi_{\theta\theta}-2\beta u_r\Pi_{\theta z}) -(3\nu+\gamma_\theta)Q_\theta-u_r\frac{dQ_\theta}{dr}\ , \tag{12b}$$

$$Q_zq_e=-\frac{\lambda_0}{\alpha}\left[\left(T\hat{C}_p\chi-\frac{u_\theta^2}{r}+3\nu u_r-\frac{u_r^2}{r}\right)\Pi_{rz} -2\beta Q_r+2\omega u_r\Pi_{\theta z}+2\beta u_r\Pi_{zz}\right] -(\gamma_z+3\nu)Q_z-u_r\frac{dQ_z}{dr}\ , \tag{12c}$$

where

$$\beta=2^{-1}\frac{du_z}{dr},\quad \omega=(2r)^{-1}\frac{d(ru_\theta)}{dr},\quad \gamma=2^{-1}r\frac{d(u_\theta/r)}{dr}\ ,$$

$$\nu=(3r)^{-1}\frac{d(ru_r)}{dr},\quad \gamma_r=2\nu-\frac{u_r}{r},\quad \gamma_\theta=-\nu+\frac{u_r}{r}\ ,$$

$$\gamma_z=-\nu,\quad \chi=\frac{d\ln T}{dr},\quad \alpha=T\hat{C}_pp,\quad q_e=\frac{\sinh\kappa}{\kappa}\ .$$

The symbol γ represents the shear rate and ω the angular speed at distance r. Note that $\gamma_r+\gamma_\theta+\gamma_z=0$, since the rate-of-strain tensor $\tilde{\gamma}$ is traceless.

On integration of (8) we obtain

$$r\rho u_r=\text{const}\ .$$

Since $u_r=0$ at the boundaries, the integration constant must be equal to zero, and we conclude $u_r=0$ everywhere in the interval $R_i\le r\le R_o$. The radial velocity gradient (du_r/dr) must also vanish. Then we can deduce from (11e) that $\Pi_{\theta z}=0$. Therefore all terms containing u_r, in the steady-state equations presented above, vanish. With these results and by using (11a)–(11f), it is also possible to show that $\beta=0$, everywhere. This in turn means $\Pi_{rz}=0$. Therefore we conclude that

$$\Pi_{\theta z}=\Pi_{z\theta}=\Pi_{rz}=\Pi_{zr}=0,\quad Q_z=0,\ \text{everywhere}\ .$$

This result considerably simplifies the steady-state equations. Since normal stress differences are measured in experiment, it is useful to define them as follows:

$$N_1=\Pi_{\theta\theta}-\Pi_{rr},\quad N_2=\Pi_{rr}-\Pi_{zz}\ .$$

There are primary and secondary normal stress coefficients associated with them. As we will see, they are generally second order in shear rate, and therefore do not manifest themselves when the shear rate is small, but become very important in the high-shear-rate regime.

C. Reduced steady-state generalized hydrodynamic equations

It is convenient to work with reduced, dimensionless generalized hydrodynamic equations when their solutions are sought after. For the purpose of reducing them, we define

$$\Delta=T_o-T_i,\quad D=R_o-R_i$$

for the temperature difference and the annular gap between the concentric cylinders, respectively. Then, with the reference variables denoted by T_r, p_r, ρ_r, U_r, η_r, and λ_r for temperature, pressure, mass density, velocity, viscosity and heat conductivity, respectively, we define the reduced variables

$$T^*=T/T_r,\quad p^*=p/p_r,\quad u^*=u_\theta/U_r\ ,$$

$$\rho^*=\rho/\rho_r,\quad \xi=r/D,\quad h^*=T\hat{C}_p/T\hat{C}_p(T_r)\ ,$$

$$\alpha^*=pT\hat{C}_p/p_rT\hat{C}_p(T_r),\quad \eta_0^*=\eta_0/\eta_r,\quad \lambda_0^*=\lambda_0/\lambda_r\ ,$$

$$\gamma^*=\gamma/(U_r/D),\quad \chi^*=\chi D,\quad \omega^*=\omega/(U_r/D)\ ,$$

$$\Pi^*=\Pi_{r\theta}/(2\eta_rU_r/D),\quad Q^*=Q_r/(\lambda_r\Delta/DT_r)\ ,$$

$$N_i^*=N_i/(2\eta_rU_r/D)\ (i=1,2),\quad Q_\theta^*=Q_\theta/(\lambda_r\Delta/DT_r)\ .$$

The reference variables are taken as follows:

$$T_r=(T_o+T_i)/2,\quad \rho_r=RT_r/p_r,\quad U_r=\Omega R_i\ ,$$

$$\eta_r=\eta_0(T_r,\rho_r),\quad \lambda_r=\lambda_0(T_r,\rho_r)\ .$$

where p_r is the initial chamber pressure taken as the reference pressure. We also define various dimensionless numbers occurring in fluid dynamics in terms of the reference variables introduced above: the Mach number,

$$\mathcal{N}_M=U_r/(\gamma_0 RT_r)^{1/2}\ ,$$

where $\gamma_0=\hat{C}_p/\hat{C}_v$ and R is the gas constant per unit mass, the Reynolds number,

$$\mathcal{N}_{\rm Re}=\rho_r U_r D/\eta_r\ ,$$

the Eckert number,

$$\mathcal{N}_E=U_r^2/\hat{C}_p\Delta,\quad [\hat{C}_p=\hat{C}_p(T_r)]\ ,$$

the Prandtl number,

$$\mathcal{N}_{\rm Pr}=\hat{C}_p\eta_r T_r/\lambda_r\ ,$$

the Knudsen number,

$$\mathcal{N}_{\rm Kn}=l/D\ ,$$

where l is the mean free path. The Reynolds number is related to the Mach and Knudsen numbers as follows:

$$\mathcal{N}_{\rm Re}=(\pi\gamma_0/2)^{1/2}\mathcal{N}_M/\mathcal{N}_{\rm Kn}\ . \tag{13}$$

It is also useful to define a composite dimensionless number δ by

$$\delta=(2\gamma_0/\pi)^{1/2}\mathcal{N}_M\mathcal{N}_{\rm Kn}=(2/\pi)\mathcal{N}_{\rm Re}\mathcal{N}_{\rm Kn}^2\ . \tag{14}$$

The first mode of expression for δ has been used in the previous papers,[2–4] but the second mode for δ provides another fluid dynamic aspect to the parameter, which we would like to discuss here. That is, since δ is a measure of the importance of nonlinear transport processes, the latter will become important to flow properties as the value of $\mathcal{N}_{\rm Re}$, $\mathcal{N}_{\rm Kn}$, or both increases.

The viscosity η_0 and thermal conductivity λ_0 are assumed to obey the density and temperature dependence obtained by Ashurst and Hoover,[1] by using a nonequilibrium molecular-dynamics method. A similar expression for viscosity was also obtained by one of us[15] by using the generalized Boltzmann equation.

By using the reduced variables defined above, we obtain the steady-state generalized hydrodynamic equations in reduced units as follows:

$$\gamma_0\mathcal{N}_M^2\frac{\rho^* u^{*2}}{\xi}=\frac{d}{d\xi}[p^*+\tfrac{1}{3}\delta(N_2^*-N_1^*)]-\delta N_1^*/\xi\ , \tag{15}$$

$$\frac{d}{d\xi}(\xi^2\Pi^*)=0\ , \tag{16}$$

$$\xi^{-1}\frac{d}{d\xi}(\xi Q^*)+2\mathcal{N}_{\rm Pr}\mathcal{N}_E\gamma^*\Pi^*=0\ , \tag{17}$$

$$\Pi^* q_e=-2\eta_0^*\gamma^*-\tfrac{2}{3}\delta(\eta_0^*\gamma^*/p^*)(2N_1^*+N_2^*)\ , \tag{18}$$

$$N_1^* q_e=4\delta(\eta_0^*\gamma^*/p^*)\Pi^*\ , \tag{19}$$

$$N_2^* q_e=-4\delta(\eta_0^*\gamma^*/p^*)\Pi^*\ , \tag{20}$$

$$\begin{aligned}Q^* q_e=&-\lambda_0^*\chi^*-(\delta/\mathcal{N}_{\rm Pr})(\lambda_0^*/\alpha^*)\\&\times[(2\gamma^*+\omega^*)Q_\theta^*\\&+\tfrac{2}{3}\mathcal{N}_{\rm Pr}(h^*\chi^*-\mathcal{N}_E u^{*2}/\xi)\\&\times(N_2^*-N_1^*)]\ ,\end{aligned} \tag{21}$$

$$\begin{aligned}Q_\theta^* q_e=&-(\delta/\mathcal{N}_{\rm Pr})(\lambda_0^*/\alpha^*)[\mathcal{N}_{\rm Pr}(h^*\chi^*-\mathcal{N}_E u^{*2}/\xi)\Pi^*\\&-\omega^* Q^*]\ ,\end{aligned} \tag{22}$$

where

$$q_e=\sinh\kappa/\kappa\ , \tag{23}$$

$$\kappa=\delta\kappa^*\ , \tag{24}$$

$$\begin{aligned}\kappa^*=&(\pi^{3/2}/\gamma_0)^{1/2}(T^{*1/4}/2\eta_0^{*1/2}p^*)\\&\times[\Pi^{*2}+\tfrac{1}{3}(N_1^{*2}+N_2^{*2}+N_1^*N_2^*)\\&+\epsilon(\eta_0^*/\lambda_0^*)(Q^{*2}+Q_\theta^{*2})]^{1/2}\ ,\end{aligned} \tag{25}$$

the reduced shear rate,

$$\gamma^*=(\xi/2)\frac{d(u^*/\xi)}{d\xi}\ ,$$

the reduced angular velocity,

$$\omega^*=(2\xi)^{-1}\frac{d(\xi u^*)}{d\xi},\quad \epsilon=\Delta/4T_r\mathcal{N}_E\mathcal{N}_{\rm Pr}\ .$$

We stress that the factor q_e is responsible for nonlinear transport processes and the reduced entropy production[7] may be defined as

$$\hat{\sigma}_{\rm ent}=\kappa\sinh\kappa\ .$$

In the limit of small κ, or small Π^*, etc. this entropy production may be approximated by $\hat{\sigma}_{\rm ent}=\kappa^2$, and thus we recover the Rayleigh-Onsager form[8] of $\hat{\sigma}_{\rm ent}$ for linear processes.

Note that the equation of continuity is omitted from the set (15)–(22), since $u_r=0$, everywhere, as we have already discussed. Therefore the equation of continuity does not show up in the set. The density is determined through the equation of state.

In the set (15)–(22) the reduced pressure p^* is defined with a reference pressure p_r, but if p^* were instead defined relative to the kinetic energy $\rho_r U_r^2/2$, and then if the relations (13) and (14) between δ, $\mathcal{N}_{\rm Re}$, $\mathcal{N}_M$, and $\mathcal{N}_{\rm Kn}$ were used, (15) in particular would have $\mathcal{N}_{\rm Re}^{-1}$ multiplied to the normal stress differences instead of $\mathcal{N}_M^2$ on the left and δ on the right. In any case, since δ is a composite number consisting of either $\mathcal{N}_{\rm Re}$ and $\mathcal{N}_{\rm Kn}$, or $\mathcal{N}_M$ and $\mathcal{N}_{\rm Kn}$, the constitutive equations (18)–(22) contain the Reynolds number, and therefore Π^*, N_1^*, N_2^*, etc. depend on $\mathcal{N}_{\rm Re}$ among other parameters. It then is interesting to see how they vary with $\mathcal{N}_{\rm Re}$ or δ at a given $\mathcal{N}_{\rm Kn}$, in the case of the cylindrical Couette flow under consideration. Since the set (15)–(22) is not possible to solve analytically, the question must be answered by a numerical solution

method. Since we have discussed the numerical method in detail in the previous papers,[2,3] we will refer the reader to them for it. We simply remark that a sixth-order Runge-Kutta method is used together with a shooting method.

It is useful to remark that the Navier-Stokes and Fourier equations[16] for the cylindrical Couette flow are

$$\gamma_0 \mathcal{N}_M^2 \frac{p^*(u^*)^2}{\xi} = \frac{d}{d\xi} p^* , \tag{26}$$

$$\frac{d}{d\xi}(\xi^2 \Pi^*) = 0 , \tag{27}$$

$$\xi^{-1} \frac{d}{d\xi}(\xi Q^*) + 2\mathcal{N}_{\mathrm{Pr}} \mathcal{N}_E \gamma^* \Pi^* = 0 , \tag{28}$$

$$\Pi^* = -2\eta_0^* \gamma^* , \tag{29}$$

$$Q^* = -\lambda_0^* \chi^* , \tag{30}$$

which arise from (15)–(22) if we set $N_1^* = -N_2^* = 0$, $Q_\theta^* = 0$, and $q_e = 1$. Note that these conditions are arrived at if the fluxes are sufficiently small, so that the terms of quadratic or higher order in the fluxes are neglected in the constitutive equations. Thus we see that the Navier-Stokes and Fourier equations are a particular case of the generalized hydrodynamic equations (15)–(22). Since η_0^* and λ_0^* are independent of the gas density, the set (26)–(30) yields, for example, Π^*, which in this particular case does not change with $\mathcal{N}_{\mathrm{Re}}$, as is easily expected from the fact that the Reynolds number does not appear in (29) and (30). We will find that this is not the case with the set (15)–(22).

If the factor q_e is retained in (29) and (30), then the shear stress and heat flux depend on the shear rate and the temperature gap, and the effective shear viscosity, for example, becomes non-Newtonian and varies with increasing shear rate or $\mathcal{N}_{\mathrm{Re}}$. This is one of the aspects we would like to show with the set (15)–(22) in this paper.

We obtain from (19) and (20) the relation

$$N_1^* = -N_2^* .$$

Therefore we may eliminate (20) from the set of generalized hydrodynamic equations to consider for the problem in hand. We also obtain from (18) and (19) the following relation between N_1^* and Π^*:

$$(N_1^* + 3p^*/2\delta)^2 + 6\Pi^{*2} = 9p^{*2}/4\delta^2 ,$$

which we call the stress ellipse. This is a generator of a cone in (Π^*, N_1^*, p^*) space, and the solutions of the generalized hydrodynamic equations must follow a trajectory confined to a sector on the cone surface. This restriction leads to the singular behavior of various fluid variables at the critical Reynolds number, as we will show in Sec. III. In fact, the discriminant of the ellipse vanishes as the Reynolds number surpasses the critical value, and the vanishing discriminant in turn provides a boundary condition for pressure. This pressure boundary condition frees one of the boundary conditions on velocity, temperature, and mass density, which we assume to be

$$u^* = 0, \quad T^* = T_i/T_r$$

at the inner cylinder wall;

$$u^* = 1, \quad T^* = T_o/T_r$$

at the outer cylinder wall; and

$$[2\pi(R_o^2 - R_i^2)]^{-1} \int_{R_i}^{R_o} dr\, 2\pi r \rho^*(r) = 1$$

for the mass density. We observe that the condition on the mass density is, strictly speaking, not a boundary condition. It simply expresses the mass conservation law. Since experiment does not provide us with a density boundary condition or a pressure boundary condition, it is the only sensible option left for us to take.

The vanishing discriminant of the stress ellipse gives the relation $p^* = 4\sqrt{2}\Pi^*\delta/3$ at the inner boundary when $\mathcal{N}_{\mathrm{Re}} \geq \mathcal{N}_{\mathrm{Re}}^c$. We replace the boundary condition on u^* at the inner boundary when $\mathcal{N}_{\mathrm{Re}} \geq \mathcal{N}_{\mathrm{Re}}^c$. We remark that the boundary conditions presented above are stick boundary conditions. More detailed discussions of the question of boundary conditions for rarefied gases are given in Ref. 3.

III. REYNOLDS-NUMBER DEPENDENCE OF FLOW PROPERTIES

Equations (15)–(22) are numerically solved, subject to the stick boundary conditions as described in Refs. 2 and 3, and flow profiles are obtained for various values of $\mathcal{N}_{\mathrm{Re}}$ at a given gas density (i.e., Knudsen number). Although we have calculated flow profiles for all the flow quantities appearing in the set (15)–(22), for lack of space we will present only those related to the velocity and stresses, since the latter are the most interesting from the viewpoint of flow instability[17] and turbulence.[18] The parameter values for various results are summarized in Table I.

In Figs. 1(a)–1(c) the reduced velocity, shear stress, and primary normal stress difference are plotted against the reduced radial distance ξ for various values of the Reynolds number indicated. The value of the Knudsen number is fixed at $\mathcal{N}_{\mathrm{Kn}} = 0.0544$. Since the secondary normal stress difference is related to the primary one by the relation $N_2^* = -N_1^*$ in the present case, we do not show the results for N_2^*. The velocity profiles show a slip on passing the critical value of $\mathcal{N}_{\mathrm{Re}}$ listed in Table I. Judged

TABLE I. Parameter values.

Curve	$\mathcal{N}_{\mathrm{Kn}}$	$\mathcal{N}_{\mathrm{Re}}$	$\mathcal{N}_M$
1	0.0544	29.73	1.00
2	0.0544	0.34	2.03
3	0.0544	69.02	2.32
4	0.0544	148.6	5.00
5	0.0544	208.1	7.00
6	0.0544	297.2	10.00

	$\mathcal{N}_{\mathrm{Kn}}$	$\mathcal{N}_{\mathrm{Re}}^c$ [a]
	0.005 44	1699.4
	0.0544	69.02
	0.544	1.397

[a]Critical values of $\mathcal{N}_{\mathrm{Re}}$.

from the trend, the velocity profile is expected to be flat and equal to zero as $\mathcal{N}_{\mathrm{Re}} \to \infty$. Closely related to this behavior of the velocity profile is the anomalous reduction in the shear stress and normal stress difference at the inner wall, which rotates at an angular velocity commensurate to the $\mathcal{N}_{\mathrm{Re}}$ value in question. Clearly, they vanish with increasing $\mathcal{N}_{\mathrm{Re}}$ over the entire gap between the cylinders. The velocity profiles do not change at the same rate as do the shear stress and normal stress difference. In order to see this point more clearly, we define the effective shear viscosity η^* and primary normal stress coefficient ψ_1^* by the relations below:

$$\eta^* = -\Pi^*/2\gamma^* , \tag{31a}$$

$$\psi_1^* = -N_1^*/\gamma^{*2} . \tag{31b}$$

These effective transport coefficients are plotted against the reduced distance ξ in Fig. 2. The maxima in the curves in Fig. 2 are due to the viscous heating effect, which increases the temperature of the gas in midstream, and thereby the Newtonian viscosity of the gas, since the latter depends on temperature such as $T^{2/3}$ in the leading term.[1-3] However, the sharp, noticeable changes in η^* and ψ_1^* in the inner boundary layer are mainly due to the velocity gradient being relatively steeper than are Π^* and N_1^* in the boundary layer. Therefore the effective viscosity changes sharply in the boundary layer, altering the dynamics of flow there. This mechanism for local change in effective viscosity *is absent in the Navier-Stokes equation* in which the shear viscosity remains constant *despite* the changing local velocity field. As a matter of fact, the concept of effective viscosity is alien to the Navier-Stokes theory, and for this reason the Navier-Stokes theory is not useful for rheology and rarefied-gas dynamics.

In Figs. 3(a) and (b) we have plotted the values of Π^* and N_1^* at the inner cylinder wall against $\log_{10}(\mathcal{N}_{\mathrm{Re}}/\mathcal{N}_{\mathrm{Re}}^c)$ for three values of $\mathcal{N}_{\mathrm{Kn}} = 0.00544$ (□), 0.0544 (+), and 0.544 (◇), where $\mathcal{N}_{\mathrm{Re}}^c$ is the critical Reynolds number beyond which the velocity slips over the inner cylinder

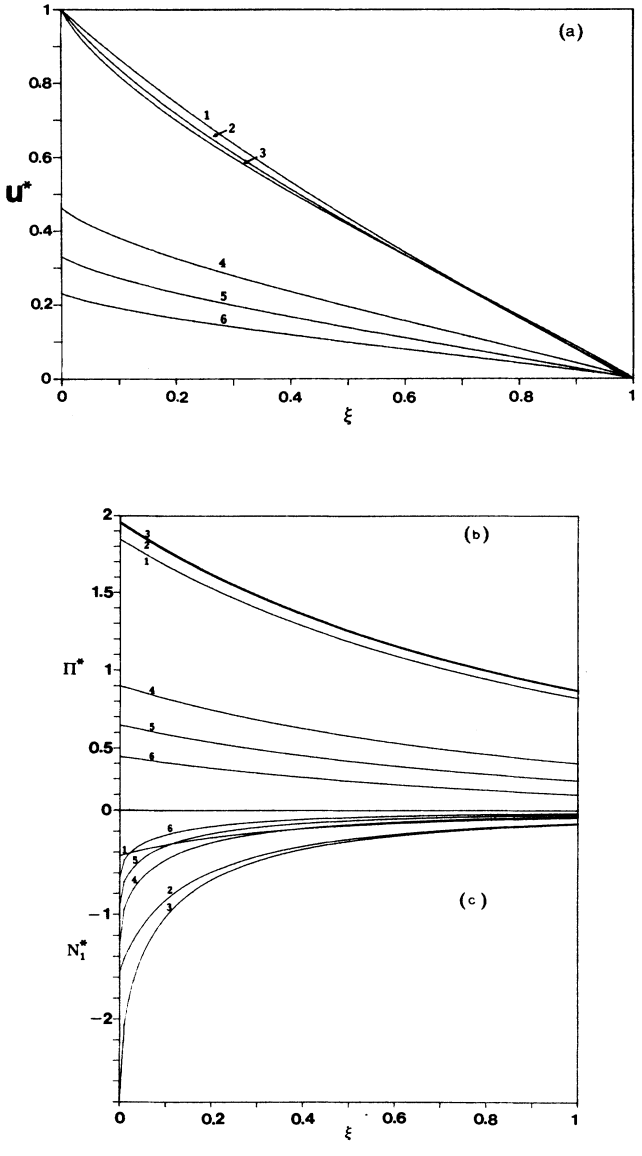

FIG. 1. (a) Velocity profiles for various values of $\mathcal{N}_{\mathrm{Re}}$. (b) Shear stress profiles for various values of $\mathcal{N}_{\mathrm{Re}}$. (c) Primary normal stress difference profiles for various values of $\mathcal{N}_{\mathrm{Re}}$. The values of $\mathcal{N}_{\mathrm{Re}}$ and the meanings of the numerals are summarized in Table I.

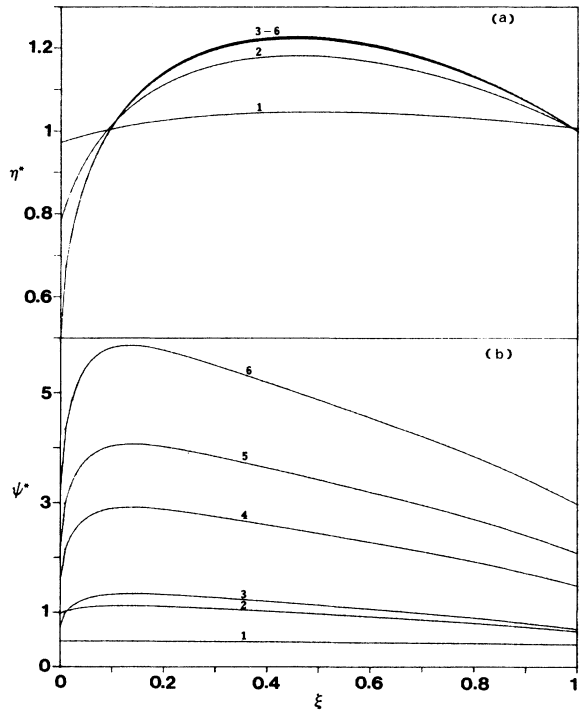

FIG. 2. (a) Effective viscosity vs ξ for various values of $\mathcal{N}_{\mathrm{Re}}$. The values of $\mathcal{N}_{\mathrm{Re}}$ are summarized in Table I. (b) Normal stress coefficient vs ξ. The numbering of the curves is the same as in other figures.

wall. The curves indicate that there is a transition (singular) point beyond which Π^* and N_1^* sharply decrease in magnitude, eventually vanishing as $\mathcal{N}_{Re}$ increases to a sufficiently large value. We find that the $\mathcal{N}_{Re}$-dependence of Π^* and N_1^* can be empirically fitted to good accuracy by the following functional forms.

(i) *Subcritical region:*

$$\Pi^* = \mathcal{N}_{Re}^{-(\alpha-1)}(a + b\mathcal{N}_{Re})^{\alpha/2} , \tag{32a}$$

$$N_1^* = \mathcal{N}_{Re}^{\beta}/[c\sinh^{-1}(f\mathcal{N}_{Re}) + d] . \tag{32b}$$

(ii) *Supercritical region:*

$$\Pi^* = a \log_{10}\mathcal{N}_{Re} + b , \tag{33a}$$

$$N_1^* = n \log_{10}\mathcal{N}_{Re} + m , \tag{33b}$$

$$\text{for } \mathcal{N}_{Kn} = 0.005\,44, \quad \text{and } \Pi^* = s/\mathcal{N}_{Re}^{\epsilon} , \tag{33c}$$

$$N_1^* = -n/\mathcal{N}_{Re}^{\beta} , \tag{33d}$$

for $\mathcal{N}_{Kn} = 0.0544$ and 0.544. The correlation coefficients of the linear regressions for the equations presented above range from 0.9988 to 0.9999, indicating good fittings. The fitting functions for $\mathcal{N}_{Kn} = 0.0544$ and 0.544 change to a simple power form from a logarithmic function holding for $\mathcal{N}_{Kn} = 0.005\,44$. Therefore there appears to be some qualitative change in dynamics on transition from $\mathcal{N}_{Kn} = 0.005\,44$ to $\mathcal{N}_{Kn} = 0.0544$. We have no explanation for this change at present, although this density (i.e., $\mathcal{N}_{Kn}$) dependence is reminiscent of that of the drag coefficient for a compressible fluid.[19]

The various parameter values in the formulas above are summarized in Table II. We have shown in a previous work[3] that the slip exhibited by the velocity and the stresses at the inner cylinder wall is due to the constraint imposed by the constitutive equations on the shear stress and the normal stress, which must remain on the stress ellipse. This constraint has led to a relationship between the pressure and the shear stress at a boundary, and this relation makes one of the boundary conditions superfluous. The velocity boundary condition at the inner cylinder wall turns out to be such a boundary condition to be removed, and the consequence is the velocity slip at the inner cylinder wall. The velocity slip necessarily gives rise to anomalous reductions in the stresses and the drag force at the inner wall. This aspect was investigated with respect to the $\mathcal{N}_{Kn}$ dependence in a previous paper.[3] Here we have presented the $\mathcal{N}_{Re}$ dependence of the behavior. We find that the slip phenomenon ap-

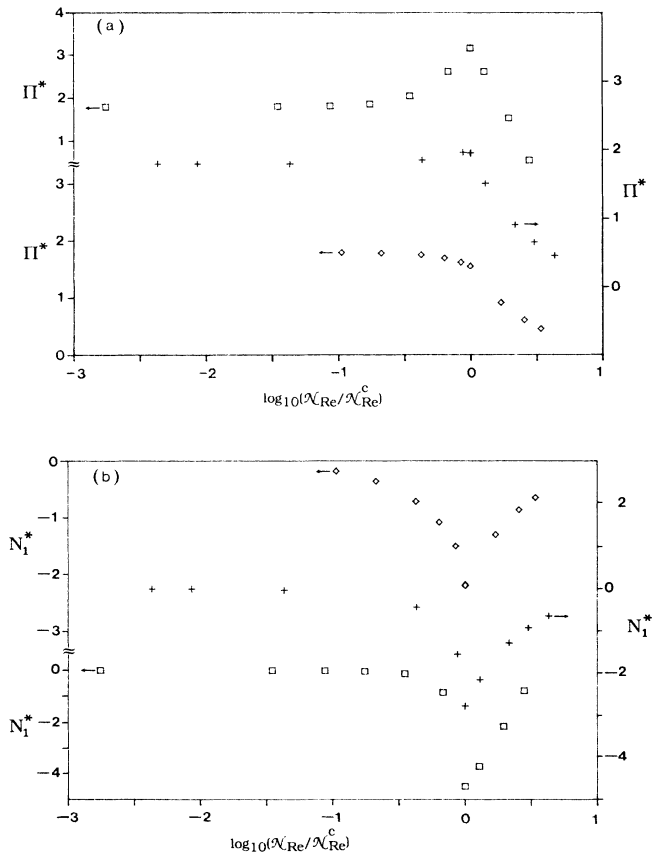

FIG. 3. (a) Shear stress at the inner cylinder wall vs $\log_{10}(\mathcal{N}_{Re}/\mathcal{N}_{Re}^{c})$. The symbols are □ for $\mathcal{N}_{Kn} = 0.005\,44$, + for $\mathcal{N}_{Kn} = 0.0544$, and ◇ for $\mathcal{N}_{Kn} = 0.544$. (b) Primary normal stress difference at the inner cylinder wall vs $\log_{10}(\mathcal{N}_{Re}/\mathcal{N}_{Re}^{c})$. The meaning of the symbols is the same as in panel (a).

TABLE II. Parameter values for fitting functions.

Subcritical

$\Pi^* = s\mathcal{N}_{Re}^{1-\alpha}(a + b\mathcal{N}_{Re})^{\alpha/2}$ [a]

$\mathcal{N}_{Kn}$	α	a	b	s
0.005 44	1.0182	10	0.014	1.0116
0.0544	1.0516	10	0.1	0.0116
0.544	1.0642	11	0.2	0.9086

$N_1^* = \mathcal{N}_{Re}^{\beta}/[c\sinh^{-1}(0.5\mathcal{N}_{Re}) + d]$

$\mathcal{N}_{Kn}$	β	c	d	f
0.005 44	0.3	−9879.82	81.8875	0.5
0.0544	0.3	−110.62	5.647 57	0.5
0.544	0	−0.199 25	0.515 63	300

$C_d = \Pi^*/\mathcal{N}_{Re}$ [a]

Supercritical

$\Pi^* = a \log_{10}\mathcal{N}_{Re} + b$; $N_1^* = n \log_{10}\mathcal{N}_{Re} + m$; $\mathcal{N}_{Kn} = 0.005\,44$

a	b	n	m
−5.88	22.21	8.315	−31.41

$\Pi^* = s/\mathcal{N}_{Re}^{\epsilon}$; $N_1^* = -n/\mathcal{N}_{Re}^{\beta}$; $\mathcal{N}_{Kn} \geq 0.0544$

$\mathcal{N}_{Kn}$	s	ϵ	β	n
0.0544	275.8	1.005	1.005	195.0
0.544	4.336	1.001	1.001	3.066

$C_d = \Pi^*/\mathcal{N}_{Re}$ [a]

[a] Π^* is the same as above.

pears as either one of $\mathcal{N}_{\mathrm{Kn}}$ and $\mathcal{N}_{\mathrm{Re}}$ is increased beyond the critical value; the two parameters appear only in the form of a composite parameter δ; and δ is associated with the nonlinear constitutive equations. These facts suggest that the origin of the slip phenomenon lies in the nonlinear constitutive equations, especially, for the stress tensor components. This observation is strengthened by the fact that the slip does not arise if the constitutive equation for the shear stress is linear and the normal stress differences vanish. (This is the case not only for the Navier-Stokes equation, but also for the fixed-frame-of-reference Maxwell model[20] for the stress tensor, which does not include the stress-shear rate coupling term $[\vec{\vec{\Pi}}\cdot\vec{\vec{\gamma}}]^{(2)}$, see Ref. 2.)

It is clear from (33) that the reduced shear and normal stresses decrease with the Reynolds number, and eventually vanish in the limit $\mathcal{N}_{\mathrm{Re}}\rightarrow\infty$, where the fluid approaches the ideal (Euler's) flow behavior. The Navier-Stokes theory in the present flow geometry, however, predicts that the reduced shear stress is independent of $\mathcal{N}_{\mathrm{Re}}$ and that the normal stress difference is equal to zero, and thus the flow will not become ideal for any Reynolds number. The present Couette-flow configuration thus turns out to be one of situations where the Navier-Stokes equation does not offer a mechanism capable of rendering the flow inviscid as $\mathcal{N}_{\mathrm{Re}}\rightarrow\infty$. This lack of mechanism for transition to ideal fluid behavior in the present geometry is essentially due to the independence of dissipative processes from convective effects vested in the inertia terms in the Navier-Stokes equation. From (26), (27), and (13) it is seen that, for a fixed Knudsen number, inertia effects grow with increasing Reynolds number, and yet the dissipative terms remains uninfluenced by the inertia terms, since the velocity and shear stress profiles can be separately solved for from (27) and (29) without invoking (26). This lack of coupling may be restored only if other terms left out are included in the Navier-Stokes equation by increasing the dimensionality of the equation; only then do the inertia and dissipative effects have an influence on each other. Unlike the Navier-Stokes equation, the generalized hydrodynamic equations, namely (15)–(22), exhibit an effective coupling between the convective and dissipative terms through the products of thermodynamic fluxes and gradients, and the nonlinear factor q_e, and such a coupling ensures the approach to ideal flow behavior in the large-Reynolds-number limit, even in the present geometry.

We have so far discussed the dependence on Reynolds number of flow properties irrespective of the position of the fluid particle (by this we do not mean a molecule in the fluid but an element of fluid volume), and the approach of the governing equations to the Euler equations. In the case of generalized hydrodynamic equations, it is possible for a local inviscid flow behavior to arise in the presence of large local thermodynamic gradients. In the case of a high shear rate (e.g., such as the one in the vicinity of a sharp boundary), the nonlinear factor q_e increases owing to the increased stresses and fluxes, and it, in turn, diminishes the value of effective transport coefficients, such as viscosity and thermal conductivity, or the stresses and heat flux. This results in a locally inviscid and non-heat-conducting fluid, owing to the feedback mechanism inherent to the nonlinear factor q_e and the inertia terms in the generalized hydrodynamic equations. This aspect is absent in the Navier-Stokes equation and its absence is a cause for the latter's weakness in dealing with systems far from equilibrium. The discussion given above is an elaboration on the remarks made in the introduction in connection with the calculation reported by Helberg and Orzsag.

The $\mathcal{N}_{\mathrm{Re}}$ dependence, as summarized in (32) and (33) and in Figs. 3(a) and (b), is essentially due to three factors: the first is the presence of the normal stresses in (15) and (18)–(20); the second is the nonlinear factor q_e present in the constitutive equations for Π^*, N_1^*, etc.; and the third is the inertia terms in the momentum balance equation and the constitutive equations. The first factor, as shown, gives rise to a stress ellipse, which the solution to (15)–(22) must always satisfy; to the sharp singular behavior exhibited by N_1^* and Π^*; and to the velocity slip. The second factor q_e further modifies the profiles from those predicted by the linear constitutive equations—i.e., the Navier-Stokes theory. This nonlinear factor q_e is intimately related to the entropy production, as indicated before, which vanishes as $\mathcal{N}_{\mathrm{Re}}$ increases to a sufficiently large value. This behavior is not possible to understand from the standpoint of linear irreversible thermodynamics, since the Rayleigh-Onsager dissipation function[8] in the linear theory increases, quadratically, with $\mathcal{N}_{\mathrm{Re}}$. However, since as long as the flow remains laminar, the nonlinear factor q_e in effect brings about, for example, diminished shear and normal stresses at high Reynolds numbers, as indicated in Fig. 2, the energy dissipation is reduced, and, consequently, the entropy production diminishes with increasing $\mathcal{N}_{\mathrm{Re}}$. There remains a question of whether or not the flow is stable at such a high Reynolds number and the energy dissipation remains of the same nature as in a laminar flow. The stability of such a flow, however, is not possible to investigate with (15)–(22), and a fuller set is required for this purpose. A study of flow stability is in progress and will be reported in the near future.

The drag coefficient is known to contain useful information on flow over a surface or a body, and its calculation presents all the salient difficulties associated with understanding the details of fluid dynamics of flow over many decades of the Reynolds number. We define the drag coefficient, as usual, by the ratio of Π^* at the surface to the area times the reference kinetic energy per unit volume of the fluid:

$$C_d=\Pi_{r\theta}A/(\rho_r U_r^2 A/2)=\Pi_{r\theta}/(\rho_r U_r^2/2)\ , \tag{34}$$

where A is the area of the surface over which the flow occurs. We will take it as the area of the inner cylinder per unit height. By using the flow profile data we have obtained, we have computed the drag coefficient at the inner cylinder wall. The result is presented in Fig. 4, where three different symbols stand for three different Knudsen numbers: $\Diamond$ for $\mathcal{N}_{\mathrm{Kn}}=0.544$, $+$ for $\mathcal{N}_{\mathrm{Kn}}=0.0544$, and $\square$ for $\mathcal{N}_{\mathrm{Kn}}=0.005\,44$. Thus they represent different states of the gas, and the drag coefficient de-

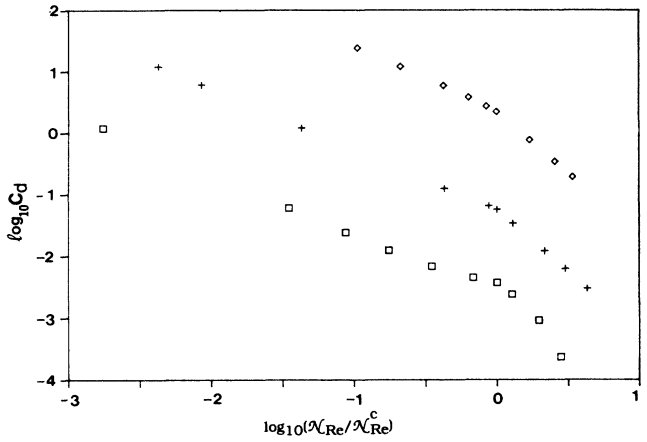

FIG. 4. Drag coefficient vs $\log_{10}(\mathcal{N}_{Re}/\mathcal{N}^c_{Re})$. The meaning of the symbols is the same as in Fig. 3.

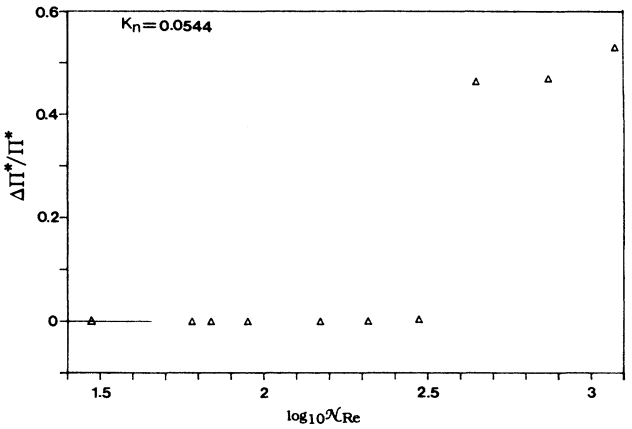

FIG. 5. $\Delta\Pi^*/\Pi^*$ vs $\log_{10}\mathcal{N}_{Re}$ in the case of $\mathcal{N}_{Kn}=0.0544$.

creases with $\mathcal{N}_{Re}$, exhibiting a drastic decrease past the critical value. It must be pointed out that the velocity slips in the postcritical region. It is then quite reasonable that the drag on the body decreases as the flow slips over the body, and thus results in a reduction in the energy dissipation due to friction. The data cover approximately three decades of $\mathcal{N}_{Re}$, and the qualitative trend is reminiscent of the $\mathcal{N}_{Re}$ dependence[19] of the drag coefficient of an incompressible fluid over a flat plate or a cylinder. We note that at high Reynolds numbers, C_d is not showing the $\mathcal{N}_{Re}^{-1}$ dependence predicted by the Navier-Stokes theory, and the deviation is again attributable to the nonlinear dissipation factor $q_e(\Pi^*, N_1^*$, etc.) and the presence of the normal stresses. By the manner of definition the drag coefficient in (34) is directly proportional to the shear stress at the inner cylinder wall. The singular behavior at the critical value of $\mathcal{N}_{Re}$ apparent in Π^* is neutralized in the case of the drag coefficient, since there is an additional factor of $\mathcal{N}_{Re}^{-1}$, and a logarithmic scale is used for the ordinate. The magnitude of the drag coefficient increases with increasing Knudsen number over the entire range of $\mathcal{N}_{Re}$. This means that the frictional force on the inner cylinder decreases at a relatively lower rate than does the kinetic energy of the flow. In other words, the dissipative effect due to friction remains dominant over the kinetic energy effect as the density is reduced.

The drag coefficient can be fitted to a function of $\mathcal{N}_{Re}$ as Π^* and N_1^* are done in (32) and (33). In fact, since C_d is proportional to Π^* itself, it is easy to find the fitting function for it. For the supercritical region,

$$C_d=(D/2\pi R_i)\Pi^*/\mathcal{N}_{Re}=(D/2\pi R_i)s\mathcal{N}_{Re}^{-\alpha}(a+b\mathcal{N}_{Re})^{\alpha/2}\ ; \tag{35a}$$

for the subcritical region,

$$C_d=(D/2\pi R_i)(a\log_{10}\mathcal{N}_{Re}+b)/\mathcal{N}_{Re}$$

$$\text{for } \mathcal{N}_{Kn}=0.005\,44 \tag{35b}$$

$$=(D/2\pi R_i)s/\mathcal{N}^c_{Re} \quad \text{for } \mathcal{N}_{Kn}\geq 0.0544\ . \tag{35c}$$

Here R_i is the radius of the inner cylinder and the parameters are given in Table II. We observe that the $\mathcal{N}_{Re}$ dependence in (35a) is similar to the empirical formula[21] used in fluid dynamics. Therefore the $\mathcal{N}_{Re}$ dependence

TABLE III. Shear stresses and drag coefficients for $q_e=1$ (Maxwell model) and $q_e\neq 1$.

$\mathcal{N}_{Re}$	Π^*	Π_m^*	C_d nonlinear	C_d Maxwell
29.72	1.85	1.85	0.124	0.124
60.34	1.96	2.00	0.065	0.066
66.49 ($\mathcal{N}^c_{Re}$)		2.02		0.061 ($q_e=1$)
69.02 ($\mathcal{N}^c_{Re}$)		1.95	0.057 ($q_e\neq 1$)	
89.17	1.51	1.50	0.034	0.034
145.6	0.90	0.90	0.012	0.012
208.1	0.65		0.006 ($q_e\neq 1$)	
297.2	0.45	0.45	0.0030	0.0030
445.9	0.205	0.30	0.000 92	0.0013
743.1	0.12	0.18	0.000 32	0.000 19
1189	0.075	0.115	0.000 13	0.000 19

above is rather suggestive as to the utility and scope of the generalized hydrodynamic equations used to calculate it.

In order to see how the nonlinear factor q_e affects the Reynolds-number dependence, we have put $q_e=1$ and calculated flow profiles. In Fig. 5 is presented the Reynolds-number dependence of $\Delta\Pi^*/\Pi^*$, where $\Delta\Pi^*=\Pi_m^*-\Pi^*$, Π_m^* and Π^* denoting the shear stress at the inner wall in the case of $q_e=1$ and $q_e\neq 1$, respectively. The numerical values for the shear stresses in Fig. 5 are presented in Table III. It must be noted that, except for the stress-shear rate coupling term $[\vec{\vec{\Pi}}\cdot\vec{\vec{\gamma}}]^{(2)}$ producing the normal stress term in (18) (see Ref. 2 for the details about this), the case of $q_e=1$ corresponds to the corotational (Jaumann derivative) Maxwell[13,22] model for the stress evolution equation. For $\mathcal{N}_{\mathrm{Kn}}=0.0544$, the model with $q_e=1$ is seen to give numerical values for the shear stress which are virtually identical with those for $q_e\neq 1$, if $\mathcal{N}_{\mathrm{Re}}\leq 208.1$, but if $\mathcal{N}_{\mathrm{Re}}\geq 208.1$, there are significant differences. These differences are expected to be more noticeable as $\mathcal{N}_{\mathrm{Kn}}$ increases, according to our previous study[3] on the $\mathcal{N}_{\mathrm{Kn}}$ dependence of flow properties. The numerical results presented here confirm again that the nonlinear factor q_e (or equivalently, nonlinear transport processes) plays an important role in determining the flow behavior in the high-$\mathcal{N}_{\mathrm{Re}}$ regime as it does in the high-$\mathcal{N}_{\mathrm{Kn}}$ regime, as shown in a previous work.[3]

IV. CONCLUDING REMARKS

The Reynolds-number dependence of shear stress and normal stress differences can indicate how the fluid responds to the external perturbation and dissipates the energy supplied to it thereby. One of the motivations for the present study is for gaining a better picture about the fluid beyond the critical Knudsen number or, equivalently, the critical Reynolds number, which is reached as the gas density diminishes. The numerical evidence indicates that the energy dissipation diminishes past the critical parameter owing to the fact that stresses become vanishingly small in the supercritical region. The behavior exhibited by the stresses beyond the critical $\mathcal{N}_{\mathrm{Re}}$ is interesting, since it indicates that the stresses are predicted to decay faster than those predicted by the Navier-Stokes theory, and thus the generalized hydrodynamic equations not only mimic the Euler equations at a smaller value of $\mathcal{N}_{\mathrm{Re}}$ than do the Navier-Stokes and Fourier equations, but also have an intrinsic feedback mechanism for locally changing the effective viscosity or the stress. The calculation indicates that there are regions in space where the viscosity is markedly diminished owing to a rapid change in the local velocity field, and in those regions the hydrodynamic equations are approximately Eulerian and nondissipative. We believe that this picture is interesting and might turn out to be useful in examining complex flows such as vortex shedding[23] and perhaps the onset[17,18] of turbulence. At this point in time the physical significance of the critical Reynolds number, especially its possible connection with turbulence, is not fully clarified. We hope to address to this question in a study on hydrodynamic instability of flow predicted by (15)–(22), which is in progress at present.

ACKNOWLEDGMENTS

We would like to acknowledge the financial support of this work by the Natural Sciences and Engineering Research Council of Canada.

---

*Also at the Physics Department, McGill University.

[1]W. T. Ashurst and W. G. Hoover, Phys. Rev. A **11**, 658 (1975).

[2]R. E. Khayat and B. C. Eu, Phys. Rev. A **38**, 2492 (1988).

[3]R. E. Khayat and B. C. Eu, Phys. Rev. A **39**, 728 (1989).

[4]R. E. Khayat and B. C. Eu, AIAA J. (to be published).

[5]The Chapman-Enskog viscosity and thermal conductivity used for normal density gases are independent of the density. See, for example, S. Chapman and T. G. Cowling, *Mathematical Theory of Nonuniform Gases,* 3rd ed. (Cambridge, London, 1970).

[6]M. N. Kogan, *Rarefied Gas Dynamics* (Plenum, New York, 1969).

[7]For more details of the entropy production and irreversible thermodynamics in connection with the generalized hydrodynamic equations used here, see (a) B. C. Eu, J. Chem. Phys. **73**, 2958 (1980); (b) **74**, 6362 (1981); (c) Ann. Phys. (N.Y.) **140**, 341 (1982); (d) J. Nonequil. Thermodyn. **11**, 211 (1986); (e) Acc. Chem. Res. **19**, 153 (1986).

[8]Lord Rayleigh, *Theory of Sound* (Dover, New York, 1949); L. Onsager, Phys. Rev. **38**, 2265 (1931).

[9]C. Hellberg and S. A. Orszag, Phys. Fluids **31**, 6 (1988).

[10](a) B. C. Eu, J. Chem. Phys. **87**, 1220 (1987); (b) B. C. Eu, Ann. Phys. (N.Y.) **118**, 187 (1979).

[11]H. Grad, Commun. Pure Appl. Math. **2**, 311 (1949).

[12]B. C. Eu, J. Chem. Phys. **82**, 3773 (1985).

[13]B. C. Eu and Y. G. Ohr, J. Chem. Phys. **81**, 2756 (1984).

[14]In Refs. 2 and 3 the steady-state constitutive equations are presented with u_r set equal to zero in anticipation of the result deduced from (8) below and the boundary conditions on u_r. The steady-state constitutive equations presented below include the terms containing u_r, which are neglected in the corresponding steady-state constitutive equations (2.12a)–(2.13c) in Ref. 2 and (2.10a)–(2.11c) in Ref. 3. We have also corrected some typographical errors inconsequential to the numerical results presented in Refs. 2 and 3. The errors do not affect the equations used for the numerical studies, namely, (15)–(22).

[15]B. C. Eu, Ann. Phys. (N.Y.) **120**, 423 (1979).

[16]L. D. Landau and E. M. Lifshitz, *Fluid Dynamics* (Pergamon, Oxford, 1959).

[17]S. Chandrasekhar, *Hydrodynamic and Hydromagnetic Stability* (Dover, New York, 1981); *Hydrodynamic Instabilities and the Transition to Turbulence,* edited by H. L. Swinney and J. P. Gollub (Springer, Berlin, 1981).

[18]J. O. Hinze, *Turbulence,* 2nd ed. (McGraw-Hill, New York, 1975).

[19]H. Schlichting, *Boundary Layer Theory,* 7th ed. (McGraw-Hill, New York, 1979).

[20]J. C. Maxwell, Philos. Trans. R. Soc. London, Ser. A **157**, 49 (1967).

[21]See, for example, B. S. Massey, *Mechanics of Fluids,* 3rd ed. (Van Nostrand, New York, 1975).

[22]It must be noted that the corotational Maxwell model for stress involves a nonlinear equation for the stress, the nonlinearity stemming only from the Jaumann derivative, unlike the generalized hydrodynamic equations which are also nonlinear in the dissipative terms and thus have the nonlinear factor q_e in them, in addition to the stress-shear rate coupling term $[\bar{\bar{\Pi}}\cdot\bar{\bar{\gamma}}]^{(2)}$. This latter term does not appear in the corotational Maxwell model for stress evolution. See Refs. 2 and 13.

[23]P. G. Saffman and G. R. Baker, Ann. Rev. Fluid Mech. **11**, 95 (1979); A. Rizzi and B. Engquist, J. Comput. Phys. **72**, 1 (1987).